FISEVIER

Contents lists available at ScienceDirect

# Materials Science in Semiconductor Processing

journal homepage: www.elsevier.com/locate/mssp



# A hybrid functional calculation of Tm<sup>3+</sup> defects in germanium (Ge)



E. Igumbor a,b,\*, W.E. Meyer a,\*

- <sup>a</sup> Department of Physics, University of Pretoria, Pretoria 0002, South Africa
- <sup>b</sup> Department of Mathematics and Physical Sciences, Samuel Adegboyega University, Km 1 Ogwa/Ehor Rd, Ogwa, Edo State, Nigeria

#### ARTICLE INFO

Article history:
Received 8 October 2015
Received in revised form
3 December 2015
Accepted 15 December 2015
Available online 19 December 2015

Keywords: Defects Formation energy Charge state

#### ABSTRACT

In this work, we present *ab-initio* calculation results for the  $Tm^{3+}$  interstitial  $(Tm_{i}^{3+})$ , vacancy-interstitial complex  $(V_{Ge}-Tm_{i}^{3+})$  and substitutional  $(Tm_{Ge}^{3+})$  defects in germanium (Ge) as determined by the density functional theory (DFT) using the Heyd, Scuseria, and Ernzerhof (HSE06) hybrid functional. We calculated the formation energies and the charge state transition levels of different configurations. Our results show that the  $Tm^{3+}$  interstitial exists in the hexagonal configuration with low formation energy. The formation energies for  $V_{Ge}-Tm_{i}^{3+}$  and  $Tm_{Ge}^{3+}$  were as low as 0.84 eV. The most energetically favourable defects were the  $V_{Ge}-Tm_{i}^{3+}$  in the *axial* configuration and the  $Tm_{Ge}^{3+}$ . The  $Tm_{Ge}^{3+}$  and  $V_{Ge}-Tm_{i}^{3+}$  introduced a single acceptor  $\varepsilon(0/-1)$  charge state transition level that was positioned deep in the middle of the band gap. The majority of the levels induced by the defects under investigation, were either shallow donor or acceptor level lying close to the band gap edges.

© 2015 Elsevier Ltd. All rights reserved.

### 1. Introduction

The application of germanium (Ge) in semiconductor material technology is attracting attention due to its high carrier mobilities [1-3]. The use of Ge technology has been successful lately due to the understanding of the role that defects play in it. The role of defects in Ge is well understood from their formation energies and transition charge state levels in the band gap. Studies of electronic properties of elemental radiation induced defects in Ge are relatively scarce and this deficiency recently led towards investigative experimenting and theoretical modelling [4–6] of defects in Ge. Deep level transient spectroscopy (DLTS) [7,8] and infrared absorption spectroscopy [9] studies have succeeded in identifying new radiation induced defects paired with impurities. Perturbed angular correlation spectroscopy (PACs) studies [10,11] have led to important findings on the mobility and electrical activities of vacancies (V) and interstitials (I); and lately, these two defects have been investigated after introduction at low temperature by in situ DLTS [7,8]. Studies of self-, di- interstitials, vacancies and substitution related defects in Ge have attracted interest in the past decades [12]. Despite the effort made so far in identifying different defects in Ge, there is still more to be accomplished. The rare earth (RE) elements are known to have a partially filled inner 4f shell which gives rise to sharp transitions that are largely insensitive to

the crystal host and temperature variations [13-15]. RE element related defects such as Tm doping of ZnO [16], and other materials have been reported [17–21]. Thulium ions (Tm<sup>3+</sup>) doped materials have been used to generate blue laser emission through non-linear up-conversion of radiation from the infrared to the visible range [17,18,22]. Recently optical properties of Tm-doped materials were studied and EL has been observed from these materials [16,23,19]. Light emission has been attributed to thulium and erbium defects in material [13-15]. Previous studies of RE implanted Si showed sharp emission peaks that were attributed to Tm<sup>3+</sup> [24]. While the Er was found in interstitial positions as well as in defect complexes [25], the cerium was found to act as an acceptor in a substitutional position in Si [26]. One would expect that Tm<sup>3+</sup> interstitials or other related defects in Ge will create deep donor levels, however experimental studies of these defects are yet to be performed. In this work, using the hybrid functional of Heyd, Scuseria, and Ernzerhof (HSE06) [27], we have carried out a detailed density functional theory (DFT) calculation of the electronic properties of Tm<sup>3+</sup> interstitial (Tm<sub>3</sub><sup>3+</sup>) in the hexagonal (H) configuration, substitutional ( $Tm_{Ge}^{3+}$ ) and vacancy–interstitial ( $V_{Ge} - Tm_i^{3+}$ ) defects in Ge with a view to finding the most stable defect types from the formation energies of the various charge states. The charge state thermodynamic transition levels were also examined to determine the type of level induced in the band gap by Tm<sup>3+</sup> defects. The rest of this paper has been organized as follows: in the next section, we present a description of the computational methodology. The results and discussion were presented in Section 3. Finally, we present our concluding remarks in Section 4.

<sup>\*</sup> Corresponding authors.

E-mail addresses: elgumuk@gmail.com (E. Igumbor),
wmeyer@up.ac.za (W.E. Meyer).

## 2. Computational details

We performed a DFT electronic structure calculation using the Vienna ab-initio Simulation Package (VASP) [28,29]. The Projectoraugmented wave (PAW) method, as implemented in the VASP code was used to separate the inert core electrons from the chemically active valence electrons [28,30]. Calculations were carried out using the Heyd, Scuseria, and Ernzerhof (HSE06) [27] hybrid functional. In this approach, the short-range exchange potential is calculated by mixing a fraction of nonlocal Hartree-Fock exchange with the generalized gradient approximation (GGA) functional of Perdew, Burke, and Ernzerhof (PBE) [31]. In contrast to the local density approximation and the generalized gradient approximation that underestimate the band gap of the semiconductor [32,33], the HSE06 functional gives an excellent description of the electronic band gap and charge state transition properties for a wide range of the defects in group-IV semiconductors [32,34.6]. For the past decades, the study and prediction of the electronic properties of materials with f orbital valence electrons was difficult due to the fact that the f orbital is highly localized. The highly localized forbitals were previously treated using LDA+U and other methods [35-38]. Recently, density functional theory using hybrid functionals has been successfully implemented, predicting the electronic and band gap properties of several materials with f orbital in the valence shell [35,39]. Following the successful implementation of the hybrid functional, it became feasible for us to handle the f state in the valence shell of  $Tm^{3+}$ . For Ge, the 4 s and 4p electrons in the outer shell were treated as valence electrons, while for Tm<sup>3+</sup>, the 6 s, 5p and 4f orbitals were considered as valence electrons. For the bulk, geometric optimization of Ge was performed on an 8-atom unit cell with an 8<sup>3</sup> Monkhorst-Pack [40] k-point Brillouin zone sampling scheme and cutoff energy of 600 eV. For the defects, we employed a 64 atom supercell using a 2<sup>3</sup> Monkhorst-Pack [40] k-point Brillouin zone sampling scheme, and we set the plane wave cutoff of the wave function expansion to 400 eV. We refined the geometry until the final change in the total energy was less than  $10^{-5}$  eV and the forces were relaxed to below 0.001 eV/Å. In all the calculations, spin orbit coupling was taken into account. The formation energy  $(E^{t})$  of defect is derived directly from total energies, allowing the calculation of equilibrium defect concentrations [41]. To calculate the defect formation and thermodynamic transition  $(\epsilon(q/q'))$  levels, we calculated the total energy E(d,q) for a supercell containing the optimized defect d in its charge state q. The defect formation energy  $E^f(d,q)$  as a function of electron Fermi energy  $(\varepsilon_F)$  is given as [42,43]

$$E^f(d,\,q) = E(d,\,q) - E(pure) + \sum_i (\triangle n)_i \mu_i + q[E_V + \varepsilon_F] + E^q_{cor}, \eqno(1)$$

where E(pure) is a supercell without a defect,  $(\triangle n)_i$  is the difference in the number of constituent atoms of type i between the

supercells,  $E_V$  is the valence band maximum (VBM) and  $\mu_i$  represents the chemical potential of different constituent atoms. Errors in  $E^f(d,q)$  due to finite-size effects within the supercell and inaccuracy underlying the approximation of the energy functional, were handled by including a correction term  $E_{cor}^q$  according to Freysoldt et al. [42,43]. The defect transition energy level  $\epsilon(q/q')$  is the Fermi energy for which the formation energy of charge state q equals that of charge state q' and is given as [42]

$$\epsilon(q/q') = \frac{E^f(d, q; \varepsilon_F = 0) - E^f(d, q'; \varepsilon_F = 0)}{q' - q} \tag{2}$$

The method proposed by Stephan et al. [44] was used for the calculation of the ionization energy ( $I_A$ ) related to the conduction band (CBM) and the electron affinity ( $E_A$ ) related to valence band maximum (VBM). The pristine Kohn–Sham band gap of Ge was calculated to be 0.80 eV, which was higher than the experimental band gap at 0 K. For consistency, we employed the quasiparticle band gap [45,44] calculation. From the calculated  $I_A$  and the  $E_A$  energies of 4.00 and 3.22 eV respectively, we obtained a Ge band gap of 0.78 eV, which is in agreement with the experimental band gap at 0 K reported by Morin et al. [46]. The binding energies  $E_b$  which are defined as the energy required to split up the defects cluster into well separated non-interacting defects were calculated using the method proposed by Zollo et al. [47]. For the  $V_{Ge}$ -Tm $_i$ <sup>3+</sup> in the axial configuration, we obtained a binding energy of 4.21 for the neutral state, showing the stability of the  $V_{Ge}$ -Tm $_i$ <sup>3+</sup> defect.

#### 3. Results and discussion

## 3.1. Structural properties and energetics of Tm<sup>3+</sup> defects in Ge

The relaxed geometric structures of Tm<sup>3+</sup> defects in Ge are shown in Fig. 1. Fig. 1(a) represent the structure of the  $Tm_i^{3+}$  in the H configuration. In this configuration, the angle between the defect atom and the nearest Ge atom before and after relaxation was 86° and 94°, respectively. The interstitial atom caused a change in atomic position after relaxation which led to a bond length reduction between the Tm and Ge atoms by 0.05 Å. The geometric structures of the  $V_{Ge}$ -Tm<sub>i</sub><sup>3+</sup> in both the axial and basal configurations are displayed in Figs. 1(b) and (c), respectively. In both configurations, after relaxation, the bond lengths between the defect atom and its two nearest Ge neighbours were reduced from 2.88 to 2.71 Å and from 3.02 to 2.92 Å. For the  $V_{Ge}$ -Tm<sub>i</sub><sup>3+</sup>, the bond angle between the Tm atom and two nearest Ge neighbours was reduced from 52.7° to 51.3°. It was interesting to note that the same change of bond length and bond angle was observed in both the axial and basal configurations except that the position of the vacancy atom differed. The geometric structure of the  $Tm_{Ge}^{3+}$  is shown in Fig. 1(d). The introduction of the substitutional defect led to structural rearrangement of the Ge crystal supercell. After the relaxation of

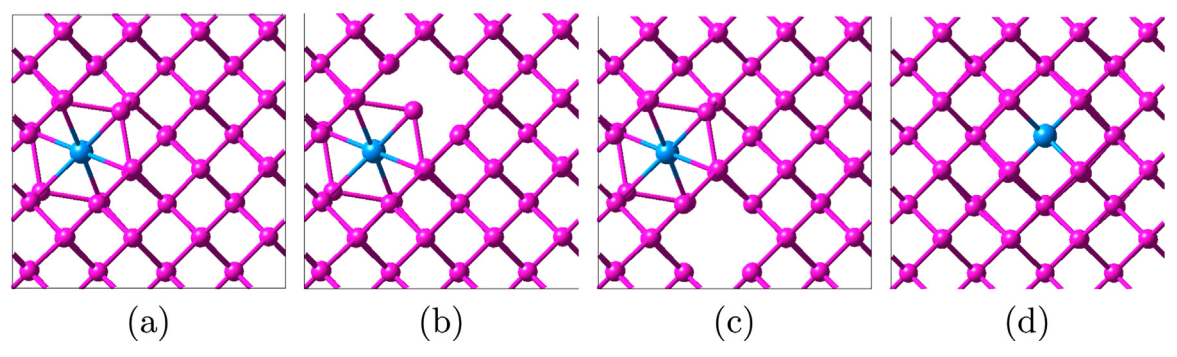


Fig. 1. The relaxed structures of  $Tm^{3+}$  defects in Ge, defect atom in blue and the wide space in the crystal structure indicating the position of the Ge vacancy; (a) H configuration of  $Tm^{3+}_i$ , (b)  $V_{Ge}$ - $Tm^{3+}_i$  (axial) (c)  $V_{Ge}$ - $Tm^{3+}_i$  (basal) and (d)  $Tm^{3+}_{Ge}$ .

# Download English Version:

# https://daneshyari.com/en/article/727930

Download Persian Version:

https://daneshyari.com/article/727930

Daneshyari.com